

## Surface boundary layer characteristics over caatinga vegetation in tropical semiarid region of N-E Brazil

S. R. PATEL<sup>(1)</sup>, M. DE FÁTIMA CORREIA<sup>(1)</sup>, A. OCIMAR MANZI<sup>(2)</sup>,  
M. B. L. OLIVEIRA<sup>(2)</sup> and M. R. DA SILVA ARAGÃO<sup>(1)</sup>

<sup>(1)</sup> *Unidade Acadêmica de Ciências Atmosféricas, Universidade Federal de Campina Grande-UFCCG - Campina Grande-PB, Brazil*

<sup>(2)</sup> *Instituto Nacional de Pesquisas da Amazônia - Manaus, Brazil*

(ricevuto il 5 Febbraio 2007; revisionato il 23 Luglio 2007; approvato il 29 Luglio 2007; pubblicato online il 5 Novembre 2007)

**Summary.** — Some characteristic features of the atmospheric surface layer over a tropical semiarid station Petrolina (9.9°S, 40.22°W, 365.5 m) in N-E Brazil, are investigated, using data collected from a micrometeorological tower of 9 m height. This study utilizes the wind, temperature, humidity and carbon dioxide (CO<sub>2</sub>) data obtained for the month of July 2004. The diurnal variation of mean parameters such as temperature, relative humidity, wind speed and CO<sub>2</sub> are studied. Turbulent statistics are computed using the eddy correlation technique, and are studied under the framework of Monin-Obukhov similarity theory with results compared with other experimental studies reported in the literature.

PACS 92.60.-e – Properties and dynamics of the atmosphere; meteorology.

### 1. – Introduction

Land-atmosphere coupling is widely recognized as a crucial component of regional-, continental- and global-scale numerical models. Predictions from these large-scale models are sensitive to small-scale surface layer processes like heat and momentum fluxes at the air-soil-vegetation interface as well as boundary layer treatments [1]. Because of the increasing awareness that tropical rain forest and continental rain forest of the Amazon basin in particular may have an important role in global climatology, there have been a number of international projects on Amazon basin in Brazil [2]. However, evaluation is still needed for the semiarid region of the North-East (N-E) of Brazil. But in this region, most of the works are confined to the energy balance using Bowen ratio method, some of which may be found in the references reported in [2]. Recently, Oliveira *et al.* [3] have studied the surface energy balance of caatinga vegetation at Petrolina, a semiarid region of N-E Brazil.

Many parts of this region are submitted to an intensive desertification process, mainly because of: the removal of the native vegetation caatinga for the use of the soil for

agriculture purposes, the substitution by other agricultural vegetation, the erosion and climate variability. Caatinga is a very important ecosystem of this region because of its extension (approximately 737000 km<sup>2</sup>, which is about 63% of the region) and population (20 million inhabitants); however, it is less investigated as compared to other ecosystems of Brazil. So it is important to study some characteristics of the surface boundary layer over caatinga vegetation in tropical semiarid region of N-E Brazil to help better understanding the physical processes controlling the surface boundary layer of the region.

## 2. – Instrumental site and data collection

The micrometeorological tower of 9 m height was constructed in the area covered with the vegetation “caatinga” of approximately 4.5 m height, with trees at a distance up to 8 meters, located in Petrolina (9°03'30.6"S; 40°19'45.1"W), N-E of Brazil. The experimental site has an area of 600 hectares. The distance of the tower from the nearest boundary of the area is 1000 m. Caatinga is heterogeneous and sparse vegetation composed of grasses, deciduous bushes and small trees with thorny vegetation, cactus and bromeliaceous. The dominant thorn vegetation is deciduous, loosing its leaves as the drought sets in, and has many xerophilous features: deep, branched roots seek and compete for water, trunks and stems tend to be woody and many stems are photosynthetic. The soil of the instrumental site is classified as Agrisol yellow (PA) with low absorption of water and poor fertility. This study utilizes the wind, temperature, humidity and carbon dioxide (CO<sub>2</sub>) data obtained for the month of July 2004. The wind velocity and direction are measured by sonic anemometer (CS8000, R. M. Young, Traverse City, Michigan, USA); while the temperature and humidity of air by the thermohydrometer (HMP45C, Vaisala, Helsinki, Finland) placed at 9 meter height. The measurements of high frequency of velocity, air temperature; concentration of water vapor and CO<sub>2</sub> are conducted by variance method, which is composed of an analyzer of CO<sub>2</sub> and H<sub>2</sub>O (LI7500, Licor, Lincoln, Nebraska, USA) and a three-dimensional sonic anemometer (CSAT3, Campbell), placed at the top of the tower. These data are read at each 0.0625 seconds (16 times per seconds) by a data logger (CRIOX, Campbell) and stored in a notebook and then processed to calculate the fluxes of sensible and latent heat; and CO<sub>2</sub>, using the turbulent covariance method. For this a FORTRAN program “Eddyinpe” was developed at Alterra, Holland; and adopted in CPTC/INPE (Centre of weather and climate prediction, Brazil) for the installation at the experimental site of Caatinga. The program calculates the turbulent fluctuations in the intervals of 30 minutes, using a series of necessary corrections following the method of Aubinet *et al.* [4]. Further details of the instrumentation and the characteristics of the instrumental site may be obtained in [3].

## 3. – Data analysis

In the present study turbulence statistics are studied under the framework of Monin-Obukhov similarity theory (MOST). According to this the scaling velocity or friction velocity ( $u_{\bullet}$ ) is defined as  $u_{\bullet} = (\overline{u'w'^2} + \overline{v'w'^2})^{1/4}$ , where the overbar and prime indicate time average and deviations from the mean values, respectively. The scaling parameters of temperature ( $T_*$ ) and humidity ( $q_*$ ) are given by  $T_* = \overline{w'T'}/u_*$  and  $q_* = \overline{w'q'}/u_*$ , respectively. The stability parameter that is appropriate for the surface layer is the dimensionless length scale  $z/L$ , where  $z$  is the height of observation and  $L$  is Monin-Obukhov length scale, given by  $L = (-u_{\bullet}^3 \overline{T_v}) / (g \kappa \overline{w'T'_v})$ , where  $\kappa$  ( $= 0.4$ ) is the von Kármán constant,  $\overline{T_v}$  is the mean absolute virtual temperature in Kelvin,  $g$  is acceleration

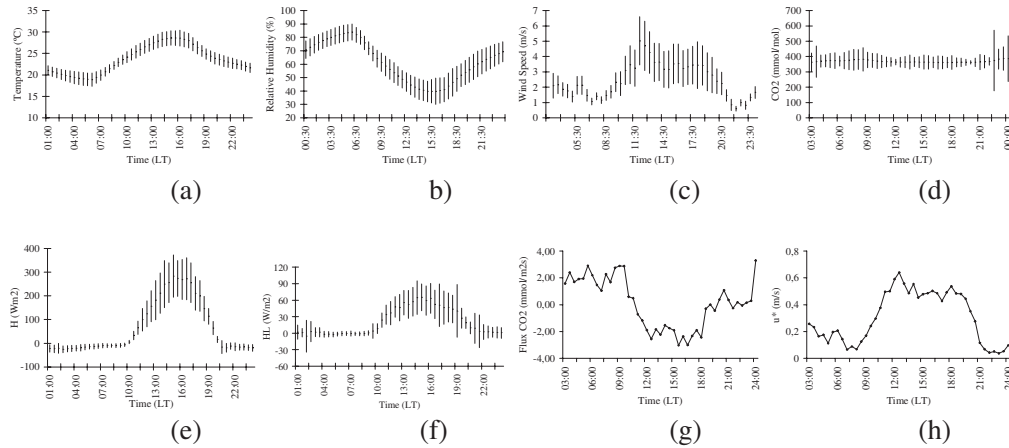


Fig. 1. – Variation with local time at 9 meter height of a) air temperature, b) relative humidity, c) wind speed, d) CO<sub>2</sub>, e) sensible heat flux, f) latent heat flux, g) flux CO<sub>2</sub> and h) friction velocity.

due to gravity and  $\overline{w'T'_v}$  is the virtual heat flux. Dimensionless standard deviations of wind components ( $\sigma_u/u_*$ ,  $\sigma_v/u_*$  and  $\sigma_w/u_*$ ) are computed using the turbulence data obtained from the instrumental tower. The vertical fluxes of sensible heat ( $H$ ) and latent heat ( $H_L$ ) are given by  $H = -\rho c_p \overline{w'T'}$ , and  $H_L = -\rho L_v \overline{w'q'}$ , where  $\rho$  is air density,  $c_p$  is the specific heat of air at constant pressure,  $L_v$  is the latent heat of vaporization of water and  $\overline{T}$  is the mean temperature. Analogously, the flux of CO<sub>2</sub> is defined as Flux CO<sub>2</sub> =  $\overline{w'\rho'_c}$ , where  $\rho'_c$  is the fluctuating part of carbon dioxide. Here, the sign reversal indicates that photosynthesis is a sink of carbon dioxide unlike evaporation, which is a source of gaseous H<sub>2</sub>O.

#### 4. – Results and discussions

##### a) Diurnal variation of mean parameters

Time averages of air temperature, relative humidity, wind speed, CO<sub>2</sub>, sensible heat flux, latent heat flux, flux of CO<sub>2</sub> and friction velocity (at 9 m level), at half hourly intervals for the month of July 2004 are plotted against local time (LT) in fig. 1 a), b), c), d), e), f), g) and h), respectively. Vertical bars in fig. 1 a), b), c), d), e) and f) represent the standard deviation from the mean. The temperatures are found to vary in the range 21.54 °C to 26.84 °C during the period of analysis. Daytime temperature variations are less and more during night. Air temperature shows a clearly defined maximum at about 1500 LT and a minimum shortly before sunrise 0530–0630 LT. The variation of humidity near the Earth's surface indicates quite well the physical processes regulating the moisture content of the air at the ground. The diurnal variation of RH (fig. 1 b) is out of phase with the temperature variation, a well-known fact. The wind velocity (fig. 1 c) is found to be maximum (5.02 m/s) at 1200 LT and minimum (0.5 m/s) at 2200 LT; and CO<sub>2</sub> (fig. 1 d) maximum (386.62 μmol/mol) and minimum (362.9 μmol/mol) at 2400 and 0300 LT, respectively. The sensible heat flux (fig. 1 e) is very commonly away from the surface in daytime conditions, approaching a minimum value during nighttime. The maximum value of sensible heat flux is at 1500 LT (283 W m<sup>-2</sup>) and minimum at 0100

TABLE I. – *Normalized standard deviations of the wind components for instability regime.*

	$\sigma_u/u_*$		$\sigma_v/u_*$		$\sigma_w/u_*$		$\sigma_u/\sigma_v$
$U > 0.5$	$3.3 \pm 1.3$	$U > 0.5$	$3.4 \pm 1.3$	$U > 0.5$	$0.6 \pm 0.2$		1.0
$U > 1.0$	$3.4 \pm 1.2$	$U > 1.0$	$3.5 \pm 1.2$	$U > 1.0$	$0.7 \pm 0.2$		1.0
$U > 2.0$	$3.6 \pm 1.0$	$U > 2.0$	$3.7 \pm 1.0$	$U > 2.0$	$0.7 \pm 0.2$		1.0
$U > 3.0$	$3.9 \pm 0.8$	$U > 3.0$	$3.9 \pm 0.9$	$U > 3.0$	$0.8 \pm 0.1$		1.0

LT ( $-22.17 \text{ W m}^{-2}$ ). It can be noted from fig. 1 f) that latent heat flux is found to be maximum at about 1430 LT ( $65 \text{ W/m}^2$ ). From fig. 1 g), the maximum and minimum fluxes of  $\text{CO}_2$  are found to be at 24 LT ( $3.50 \mu\text{mol/m}^2 \text{ s}$ ) and at 03 LT ( $-3.00 \mu\text{mol/m}^2 \text{ s}$ ) at 1500 LT, respectively. The daily variation of friction velocity is shown in fig. 1 h), which has maximum and minimum values at 1200 LT ( $0.65 \text{ m/s}$ ) and 2300 LT ( $0.9 \text{ m/s}$ ), respectively.

#### b) Turbulence statistics

In general, the MOST is a good tool for explanation of the turbulent characteristics of lower atmosphere at an observational site. According to this theory, the non-dimensional standard deviations of  $u$ ,  $v$ , and  $w$  components of wind normalized by friction velocity ( $u_*$ ) are universal functions of stability parameters ( $z/L$ ) in horizontally homogeneous and steady flow. Wyngaard *et al.* [5] and Kaimal *et al.* [6] showed that the values of  $\sigma_w/u_*$  tend to follow similarity relations irrespective of the terrain. But, Roth [7] reported that  $\sigma_w/u_*$  and stability  $z/L$  varies with observational site. Further, Roth [7] and Yersel and Goble [8] showed that the normalized standard deviations decrease with an increase of roughness length ( $z_0$ ) and that the influence of roughness on horizontal components of wind deviation is larger than that on the vertical component.

In near neutral conditions, similarity theory indicates that the normalized standard deviations of wind speed  $\sigma_{u,v,w}/u_*$  are constant with height. But the constant value is different for each wind component [7, 9].

The values of  $\sigma_{u,v,w}/u_*$  for all wind components are shown in tables I and II for the instability and stability regimes, respectively; for different wind speeds ( $> 0.5$ ,  $> 1.0$ ,  $> 2.0$  and  $> 3.0 \text{ m/s}$ ).

Comparisons of standard deviations of  $\sigma_{u,v,w}/u_*$  for instability and stability conditions are shown in table III. It can be seen from tables I, II and III that the values of

TABLE II. – *Normalized standard deviations of the wind components for stability regime.*

	$\sigma_u/u_*$		$\sigma_v/u_*$		$\sigma_w/u_*$		$\sigma_u/\sigma_v$
$U > 0.5$	$2.0 \pm 1.3$	$U > 0.5$	$2.1 \pm 1.4$	$U > 0.5$	$0.4 \pm 0.2$		0.9
$U > 1.0$	$2.1 \pm 1.3$	$U > 1.0$	$2.2 \pm 1.4$	$U > 1.0$	$0.5 \pm 0.3$		1.0
$U > 2.0$	$2.9 \pm 1.3$	$U > 2.0$	$2.9 \pm 1.3$	$U > 2.0$	$0.7 \pm 0.2$		1.0
$U > 3.0$	$3.9 \pm 1.5$	$U > 3.0$	$3.7 \pm 1.7$	$U > 3.0$	$0.8 \pm 0.2$		1.0

TABLE III. – Comparison of standard deviations of velocity components normalized by friction velocity for all stability conditions.

	$\sigma_u/u_*$	$\sigma_v/u_*$	$\sigma_w/u_*$	$\sigma_u/\sigma_v$
$z/L < 0$	3.5	3.6	0.7	1.0
$z/L > 0$	2.7	2.7	0.6	1.0

the normalized standard deviations are similar to those found in the literature, slightly different; because the values reported in this study consider the full stability range, while the other results are for the near neutral conditions only. The aim to report the values of the normalized standard deviation for full stability range and also for different values of the wind speed ( $> 0.5$ ,  $> 1.0$ ,  $> 2.0$  and  $> 3.0$  m/s) is because they can also be applied to the air pollution problems for the low or calm winds ( $< 2$  m/s) and the windy winds ( $> 2.0$  m/s) conditions. Panofsky and Dutton [9] have summarized the values of normalized standard deviations of the wind components from different experiments from different places and reported the mean values as 2.40, 1.90 and 1.25 for  $\sigma_u/u_*$ ,  $\sigma_v/u_*$  and  $\sigma_w/u_*$ , respectively and for other rolling terrain up to 4.50, 3.80 and 1.24. Zhang *et al.* [10] have reported the corresponding values based on the same instrumentation, data acquisition and data processing system, for the Gobi desert (surface roughness  $z_0 = 0.0012$  m) site as: 2.62, 2.39, 1.22; grassland ( $z_0 = 0.028$  m) site as: 2.29, 2.12, 1.18; and suburban ( $z_0 = 0.37$  m) site as: 1.95, 1.36, 1.20. Their values for  $\sigma_u/\sigma_v$  for these corresponding sites are 1.096, 1.080 and 1.434, respectively, while the results for the site of the present study are 3.522, 3.627, 0.697 and 0.970 (for  $z/L < 0$ ); and 2.709, 2.728, 0.614 and 0.983 (for  $z/L > 0$ ) for  $\sigma_{u,v,w}/u_*$  and  $\sigma_u/\sigma_v$ , respectively. Further Zhang *et al.* [10] have reported that the values of  $\sigma_{u,v}/u_*$  decrease with increase of roughness although the observational height may also be a factor and that the value of  $u_*$  decreases with decrease of roughness length or increase of measurement height. Ramana *et al.* [11] have studied the normalized standard deviations for different seasons (the hot summer or pre-monsoon season from March to May, the south-west monsoon season from June to September, the warm dry or post-monsoon season from October to November and the winter or north-east monsoon season from December to February) periods and have reported their corresponding values for different wind velocities ( $U > 0.5$ ,  $> 1.0$ ,  $> 1.5$  m/s); and shown that for the near neutral stratification the turbulence statistics are nearly independent of season. Their values for the standard deviations (for  $u$ ,  $v$  and  $w$  components) averaged for four seasons are  $2.63 \pm 0.36$ ,  $2.19 \pm 0.06$  and  $1.0 \pm 0.04$ , respectively. For the South American Pampa, Moraes [12] found the values as: 2.42, 2.78 and near unity for  $u$ ,  $v$  and  $w$  components, respectively, for near neutral condition. Wang and Mitsuda [13] have reported the values of 2.65, 2.22, 1.21 and 1.194 for  $\sigma_u/u_*$ ,  $\sigma_v/u_*$ ,  $\sigma_w/u_*$  and  $\sigma_u/\sigma_v$ , respectively in neutral stratification. So, observing the uncertainties of the values of  $\sigma_{u,v,w}/u_*$  [9, 12, 14], the results obtained in this paper, which are for the full range of stability, are consistent with the results found in the literature. In the absence of such experimental results over caatinga vegetation in the semiarid tropical region of N-E Brazil, the results of this study could not be compared. The verification of the MOST for the normalized standard deviations for the wind components, temperature, humidity and CO<sub>2</sub> are being analyzed and will be presented very soon in a separate paper. It is hoped that the results obtained in this study are useful to help better under-

standing the physical processes controlling the surface boundary layer of the region for the applications, among others, in the numerical weather and climate prediction models of the region.

\* \* \*

The INPE (Instituto de Pesquisa Espaciais) and the EMBRAPA (Empresa Brasileira de Pesquisa Agropecuária) for providing the micrometeorological data and the CNPq (Conselho Nacional de Desenvolvimento Científico e Tecnológico) for the financial support (Processo Número 504189/2003) are acknowledged.

#### REFERENCES

- [1] GARRAT J. R., *J. Climate*, **6** (1993) 419.
- [2] PATEL S. R., DA SILVA E. M., CORREIA M., DE FATIMA and COSTA A. M. N., *Nuovo Cimento C*, **28** (2005) 19.
- [3] OLIVEIRA M. B. L., SANTOS A. J. B., MANZI A. O., ALVALÁ R. C. S., CORREIA M. DE FATIMA and MOURA M. S. B., *Rev. Bras. Meteorol.*, **21** (2006) 378.
- [4] AUBINET M., GRELE A., IBROM A., RANNIK U., MONCRIEFF J. B., FOKEN T., KOWALSKI A. S., MARTIN P. H., BERBIGIER P., BERNHOFER C., CLEMENT R., ELBERS J. A., GRANIER A., GUNWALD T., MORGENSTERN K., PILEGAARD K., REBMANN C., SNIJDERS W., VALENTINI R. and VESALA T., *Adv. Ecol. Res.*, **30** (2000) 113.
- [5] WYNGAARD J. C., COTÉ O. R. and IZUMI Y., *J. Atmos. Sci.*, **28** (1971) 1171.
- [6] KAIMAL J. C., EVERSOLE R. A., LENSCHOW D. H., STANKOV B. B., KAHN P. H. and BUSINGER J. A., *J. Atmos. Sci.*, **39** (1982) 1198.
- [7] ROTH M., *Q. J. R. Meteorol. Soc.*, **119** (1993) 1105.
- [8] YERSEL M. and GOBLE R., *Boundary-Layer Meteorol.*, **37** (1986) 271.
- [9] PANOFKY H. A. and DUTTON J. A., *Atmospheric Turbulence* (A Wiley-Interscience Publication, John Wiley and Sons, New York) 1984, p. 160.
- [10] ZHANG H., CHEN J. and PARK S., *Boundary-Layer Meteorol.*, **100** (2001) 243.
- [11] RAMANA M. V., KRISHNAN P. and KUNHIKRISHNAN P. K., *Boundary-Layer Meteorol.*, **111** (2004) 153.
- [12] MORAES O. L. L., *Boundary-Layer Meteorol.*, **96** (2000) 317.
- [13] WANG J. M. and MITSUDA Y., *J. Meteorol. Soc. Jpn.*, **69** (1991) 587.
- [14] SORBJAN Z., *Structure of the Atmospheric Boundary Layer* (Prentice Hall, New Jersey, USA) 1989, p. 76.